

# Powering a Microprocessor by Photosynthesis

P. Bombelli<sup>1,2†</sup>, A. Savanth<sup>3†</sup>, A. Scarampi<sup>1†</sup>, S.J.L. Rowden<sup>1†</sup>, D. H. Green<sup>4</sup>, A. Erbe<sup>5</sup>, E. Årstøl<sup>6</sup>, I. Jevremovic<sup>5</sup>, M. F. Hohmann-Marriott<sup>6,7</sup>, P. Trasatti<sup>2</sup>, E. Ozer<sup>3\*</sup> and C.J. Howe<sup>1\*</sup>.

## Affiliations:

<sup>1</sup>Department of Biochemistry, University of Cambridge, Hopkins Building, Tennis Court Rd, Cambridge CB2 1QW, United Kingdom.

<sup>2</sup>Department of Environmental Science and Policy, Università degli Studi di Milano, Via C. Golgi, 19, 20133 Milano, Italy.

<sup>3</sup>Arm Ltd, 110 Fulbourn Rd, Cambridge, CB1 9NJ, United Kingdom.

<sup>4</sup>Culture Collection of Algae and Protozoa, Scottish Association for Marine Science, Oban, Argyll, PA73 1QA, United Kingdom.

<sup>5</sup>Department of Materials Science and Engineering, NTNU, Norwegian University of Science and Technology, 7491 Trondheim, Norway.

<sup>6</sup>Department of Biotechnology and Food Science, NTNU, Norwegian University of Science and Technology, 7491 Trondheim, Norway.

<sup>7</sup>United Scientists CORE Ltd, 2 Tewsley St., Ōtepoti Dunedin, Aotearoa New Zealand.

\*Corresponding authors. Email: [ch26@cam.ac.uk](mailto:ch26@cam.ac.uk), [emre.ozar@arm.com](mailto:emre.ozar@arm.com)

†These authors contributed equally to this work.

30 **Abstract**

31 Sustainable, affordable and decentralised sources of electrical energy are required to power the  
32 network of electronic devices known as the Internet of Things. Power consumption for a single  
33 Internet of Things device is modest, ranging from  $\mu\text{W}$  to  $\text{mW}$ , but the number of Internet of Things  
34 devices has already reached many billions and is expected to grow to one trillion by 2035, requiring  
35 a vast number of portable energy sources (*e.g.*, a battery or an energy harvester). Batteries rely  
36 largely on expensive and unsustainable materials (*e.g.*, rare earth elements) and their charge  
37 eventually runs out. Existing energy harvesters (*e.g.*, solar, temperature, vibration) are longer  
38 lasting but may have adverse effects on the environment (*e.g.*, hazardous materials are used in the  
39 production of photovoltaics).

40 Here, we describe a bio-photovoltaic energy harvester system using photosynthetic  
41 microorganisms on an aluminium anode that can power an Arm Cortex M0+, a microprocessor  
42 widely used in Internet of Things applications. The proposed energy harvester has operated the  
43 Arm Cortex M0+ for over six months in a domestic environment under natural light. It is  
44 comparable in size to an AA battery, and is built using common, durable, inexpensive and largely  
45 recyclable materials.

46  
47  
48  
49  
50  
51  
52  
53  
54  
55  
56  
57  
58  
59  
60

## 61 **Introduction**

62 The Internet of Things (IoT) comprises a vast network of small computational devices deployed  
63 in domestic, commercial, industrial and natural environments, connected to a myriad of “things”  
64 for sensing and transmitting their status, responding and communicating accordingly. This network  
65 has revolutionised many aspects of the modern world and will transform information exchange in  
66 smart homes, cities, factories, farms and natural environments<sup>1-3</sup>. The IoT is growing rapidly. With  
67 several billion IoT devices already in existence<sup>4</sup>, it is expected to reach one trillion by 2035<sup>5</sup>. Many  
68 IoT devices consume power in the range of  $\mu\text{W}$  to  $\text{mW}$ , and are frequently powered by a battery.  
69 However, powering one trillion IoT devices by lithium-ion batteries, would require 109,000 tonnes  
70 of lithium, three times more than the world’s annual production in 2017<sup>6</sup>, and not sustainable.  
71 Other battery types would also require major use of natural resources, or routine recharging and  
72 eventual replacement with inevitable negative environmental impact<sup>7,8</sup>. Consequently, energy  
73 harvesting - rather than energy storage - is desirable for powering IoT devices<sup>9</sup>. The ideal energy  
74 harvesting system must deliver sufficient power for continuous sensing<sup>10</sup>, and should be built using  
75 inexpensive and common materials, avoiding toxic components.

76 To date, examples of energy harvesting systems for IoT devices include photovoltaics (PV)<sup>11</sup>,  
77 microbial fuel cells (MFC)<sup>12</sup>, and other micro-scale energy harvesting materials<sup>13</sup>. PV are arguably  
78 the most studied, developed and perhaps most immediately practicable<sup>14</sup>. However, they do not  
79 provide power during dark periods. Microbial fuel cells (MFCs) use bacteria to oxidize a chemical  
80 fuel and generate electrical energy<sup>15</sup>. Although they can operate in the dark, MFCs depend on the  
81 metabolism of heterotrophic bacteria and require a supply of organic matter<sup>16</sup>. Photosynthetic  
82 microorganisms can be used instead of heterotrophic bacteria in the anodic chamber of these  
83 biological fuel cells. Such devices are often referred to as biophotovoltaics (BPV) as the electric  
84 current is ultimately based on electrons liberated from water through photosynthetic photolysis of  
85 water<sup>17-19</sup>. This removes the need to supply the device with organic matter as chemical fuel, and  
86 uses solar energy to drive it. One of the key components in BPV devices is the anode, which  
87 channels the current generated by the microorganisms into an external circuit. The ideal anode  
88 must be biocompatible, with adequate electric conductivity and optical properties to permit current  
89 flow and light diffusion. For BPV devices to be implemented at large scale, the anode should be  
90 durable and use abundant and low-cost materials<sup>20-21</sup>.

91 Here, we report the development of a novel aluminium-anode bio-photo-voltaic system (Al-BPV)  
92 with as photo-active component the commonly used model photosynthetic bacterium  
93 *Synechocystis sp.* PCC6803 (hereafter referred to as *Synechocystis*). The system was built in a  
94 small form factor (*i.e.*, small size) using common, durable, and recyclable materials. The system  
95 successfully and continuously powered for over six months a microprocessor based on an Arm  
96 Cortex M0+ central processing unit (CPU), one of the most commonly used CPUs found already  
97 in many commercial IoT applications. The test was conducted in a domestic environment without  
98 any dedicated artificial lighting system, additional battery or organic fuel supplement. The  
99 mechanism of operation of the Al-BPV system was studied using electrochemistry (cyclic  
100 voltammetry, potentiodynamic sweep and electrochemical impedance spectroscopy), microscopy,  
101 and microbiological characterisation.

102 This study demonstrates the robustness and practicability of an Al-BPV as a durable and reliable  
103 source of renewable power for untethered applications, paving the way for the large-scale  
104 implementation of photosynthetically powered micro-electronics.

105

106

## 107 **Results and Discussion**

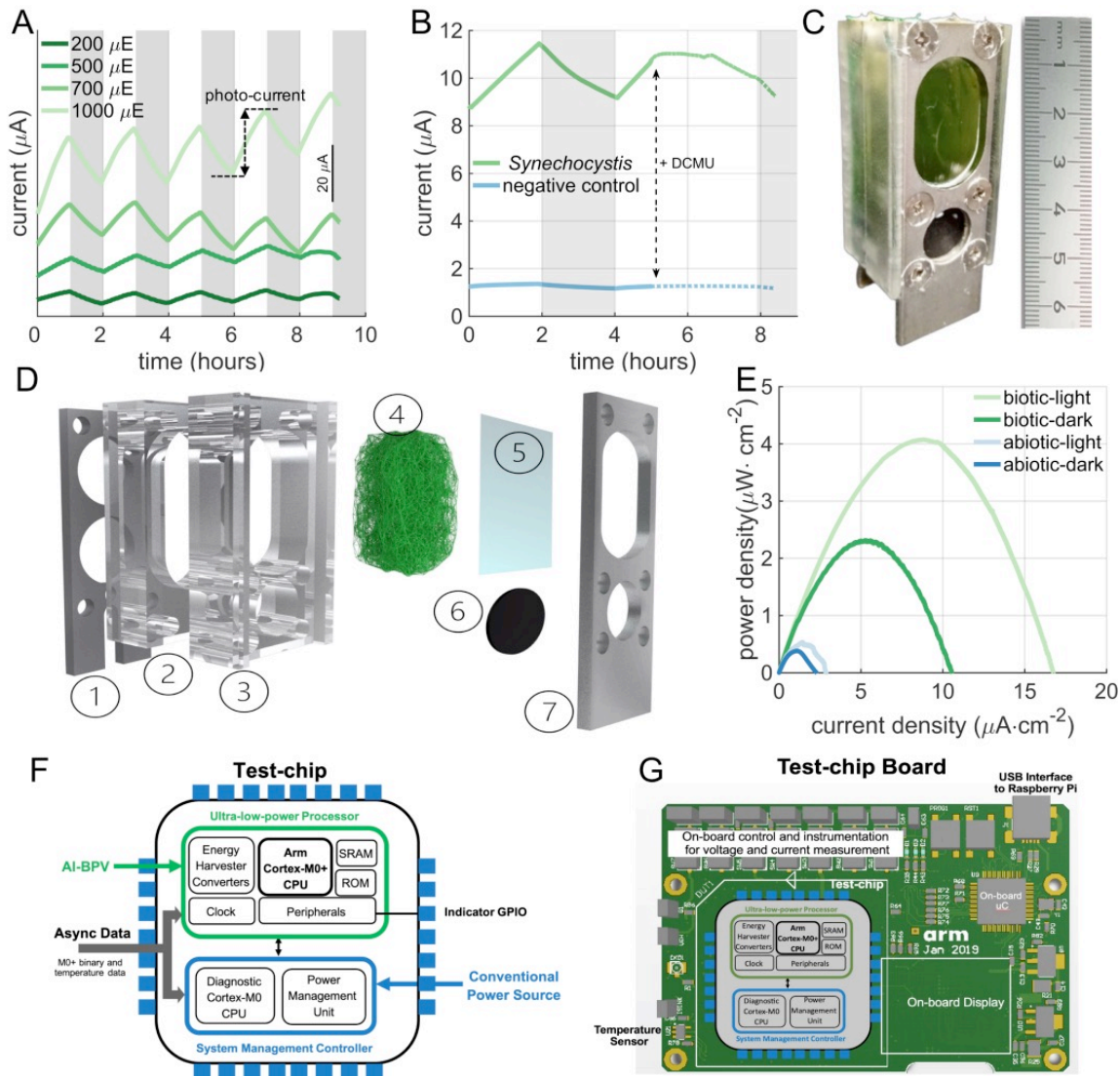
### 108 ***Rationale for using aluminium as anode***

109 To select an optimal anodic material to be used in photosynthetically driven electrochemical  
110 systems, aluminium was considered because it is one of the most abundant metals in the Earth's  
111 crust, available in large quantity as waste in the environment, and classified as not toxic<sup>22</sup>. The use  
112 of an aluminium anode in electrical energy generation systems has been described before, in  
113 aluminium-air batteries (AAB)<sup>23</sup>. In these, electrochemical aluminium oxidation in an alkaline  
114 medium is combined with oxygen reduction at the cathode. To our knowledge, the effect of  
115 introducing biological components into AAB has not been studied. Several studies have examined  
116 the physiological effects of aluminium on plants, cyanobacteria and microalgae, with results  
117 depending on the organism considered<sup>24-25</sup>. We tested growth of *Synechocystis* cultures in the  
118 presence of metallic aluminium, and found that they reached a cell density similar to control  
119 samples without aluminium (**Fig.S1**), suggesting that aluminium is biocompatible with  
120 *Synechocystis*.

121

### ***Light-dependent power production from a prototype Al-BPV***

We built a prototype BPV system (Al-BPV) using aluminium wool as anode (**Fig.S2**), with a commercial open-air cathode, stainless steel electric connectors and plastic vessels (**Fig.S3**). The prototype Al-BPV system was inoculated with *Synechocystis* (**Fig.S4A**), and first tested in a laboratory-controlled environment. The system gave peak power density of  $0.2 \mu\text{W cm}^{-2}$  and  $0.37 \mu\text{W cm}^{-2}$  under dark and light conditions respectively, indicating a photoactive component to power production. These figures were significantly greater than those observed in an abiotic negative control (**Fig.S4B**). The effect of illumination on the electrical output observed here in the prototype Al-BPV system is not seen in AABs, which are not photo-active when illuminated with visible light<sup>26</sup>, although in AABs a modest increase in the power output in response to light might be observed because of the thermal effect of illumination<sup>27</sup>. Thus, the presence of a much bigger photo-effect in the presence of *Synechocystis* compared to the abiotic control (**Fig.S4B**), and the large increase in amplitude in response to increased light intensity (**Fig.1A**) indicate that current production depends on the photo-active component of the system, (*i.e.*, the photosynthetic microorganisms). The effect of adding the photosynthesis inhibitor 3-(3,4-dichlorophenyl)-1,1-dimethylurea (DCMU)<sup>28</sup> to the anodic chamber was tested. DCMU addition had an immediate effect on photo-current (**Fig.1B**), which stopped increasing and then decreased. The effect of inactivating the photosynthetic microorganisms was tested by autoclaving the inoculated anode. This abolished autofluorescence, indicating loss of photosynthetic activity, and resulted in almost complete loss of light-dependent current (**Fig. S5**). These observations indicate that current production from the Al-BPV depends on the biological activity of the microorganisms.



149

150

151

152

153

154

155

156

157

158

159

160

161

162

163

**Fig. 1. Development and characterisation of the prototype and compact AI-BPV systems, and diagrams of the Arm Cortex-M0+ processor in a test-chip and board.** **A)** Chronoamperometry for the prototype AI-BPV system under 2 hours dark/light cycles. Effect of increasing light intensities on the photo-current. **B)** Effect on photocurrent for the prototype AI-BPV system of addition of the photosynthetic inhibitor DCMU (35  $\mu\text{M}$ ), including for the abiotic negative control with BG11 medium only (blue). **C)** Photograph of the compact AI-BPV system. **D)** 3D exploded diagram of the compact AI-BPV system. The diagram shows two stainless steel metal plates (1 and 7), an acrylic compartment made of two parts (2,3), an aluminium anode colonised with photosynthetic microorganisms (4), a Teflon gas-permeable membrane (5) and an open air cathode (6). Stainless-steel screws are not shown in this diagram. **E)** Power curve for the compact AI-BPV system and abiotic negative control (BG11 only) (scans at rate of  $0.1 \text{ mV s}^{-1}$ ). **F,G)** Schematic diagrams of the test-chip and its board. The test-chip includes two blocks: an ultra-low-power processor consisting of an Arm Cortex-M0+ CPU, SRAM, ROM, clock, peripherals, and energy harvesting converters, and a system management controller consisting of a diagnostic Arm Cortex-

164 M0 CPU and a power management unit. The AI-BPV powers the ultra-low-power processor whilst  
165 the system management controller is powered by a USB power source. The test-chip board con-  
166 tains the test-chip, a temperature sensor, voltage and current measurement circuitry, a microcon-  
167 troller taking the voltage, current and temperature measurements, a display and a USB interface to  
168 an external Raspberry Pi. The Arm Cortex-M0+ requires a minimum of 0.3  $\mu\text{W}$  (at 0.3V) to run  
169 its computational work at a frequency of 10 kHz. The minimum power consumption drops to 0.24  
170  $\mu\text{W}$  during the standby mode when computations are not running. The system management con-  
171 troller in the test-chip was powered by a conventional USB power source.

172

173

### 174 *Developing a compact AI-BPV for powering the Arm Cortex-M0+ in a domestic environment*

175 Having demonstrated the possibility of power generation in an AI-BPV system, we constructed a  
176 compact version with a small form factor, similar in size to an AA battery, referred to as the  
177 compact AI-BPV (**Fig.1C-E** and **Fig.S6,7**). Characterisation in a controlled laboratory  
178 environment (**Fig.S8**) showed a peak power density of 4.2  $\mu\text{W cm}^{-2}$  and an output maintained for  
179 over 20 days. This should be sufficient to power a real-world device, such as the Arm Cortex-M0+  
180 CPU<sup>29</sup>. This is a programmable 32-bit RISC microprocessor, highly energy- and area-efficient,  
181 supporting the ARMv6-M Thumb instruction set (**Fig.1F**). The Arm Cortex-M0+ is used in many  
182 microcontrollers and embedded applications that can run programs written in high-level  
183 programming languages. In the experiments, we used a test-chip designed and implemented by  
184 Arm<sup>30-31</sup> comprising the Arm Cortex-M0+ and a system management controller (**Fig.1G**).

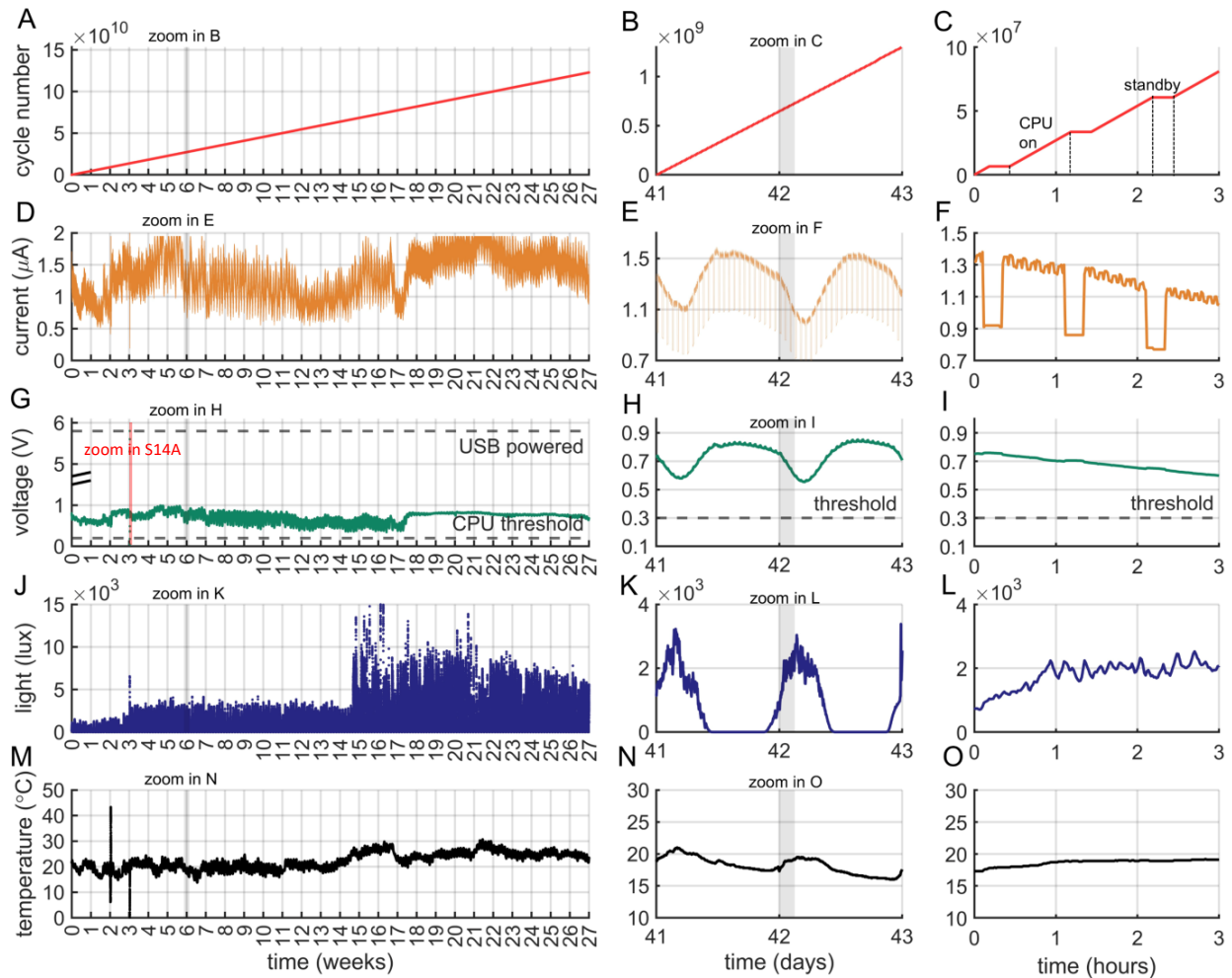
185 We programmed the Cortex-M0+ CPU to calculate a sum of consecutive integers ( $S_n$ ) as an  
186 example compute workload, and assess the correctness of the computation by verifying the sum  
187 against a precomputed value ( $S_n = \frac{n(a_1+a_n)}{2}$ ). We programmed the CPU to perform 45 minutes of  
188 computation work followed by 15 minutes of standby (**Fig.S9**).

189 The test was conducted over half a year in a domestic setting in Cambridge (UK), with ambient  
190 light as the energy input (**Fig.S10**). The anode-to-cathode voltage, current, ambient temperature  
191 and light were measured by the electronics built in the test-chip board and then recorded and  
192 visualised on the cloud-based platform ThingSpeak<sup>TM</sup> via a Raspberry-pi/router (**Figures 2 and**  
193 **S11**). During the test, the Arm Cortex-M0+ processor performed a total of 1.23E+11 cycles,  
194 resulting in a linear and continuous increase in the number of calculations performed over time  
195 (**Fig.2A-C**). Throughout the test, the Arm Cortex-M0+ processor drew an average current from

196 the compact Al-BPV of  $1.4\pm 0.4$   $\mu\text{A}$  with a voltage of  $0.72\pm 0.14$  V (**Fig.2D-I**). The light profile  
197 displayed the expected diurnal cycle (**Fig. 2J-L**) with ambient temperature ranging from a  
198 minimum of  $13.8$   $^{\circ}\text{C}$  to a max of  $30.7$   $^{\circ}\text{C}$  (**Fig. 2M-O**). As the average power drawn from the  
199 compact Al-BPV during the 27 weeks of experimental run ( $1.05$   $\mu\text{W}$ ) was larger than the minimum  
200 power required to run the CPU (i.e.,  $0.3$   $\mu\text{W}$ ), it is likely that a smaller power-generating system  
201 could be used, or that more computationally intensive algorithms could be performed.

202 The system was set up so that if the CPU failed, e.g., the compact Al-BPV cannot supply minimum  
203 operating power, the processor would automatically be switched to the mains electricity (USB  
204 powered). This would be displayed by recording a voltage  $>5\text{V}$ , and the system would need to be  
205 reset. To test this, we deliberately induced failure (for about 90 minutes at the end of the third  
206 week) by positioning an ice-pack near the temperature probe mounted on the test-chip which  
207 caused a localised lowering of the ambient temperature below  $5$   $^{\circ}\text{C}$  (**Fig.2M** red background),  
208 which is much below the minimum operating temperature  $13.8$   $^{\circ}\text{C}$ , without varying the  
209 temperature experienced by the compact Al-BPV. In this instance, the software controlling the  
210 operation of the CPU triggered to switch the power of the CPU from the Al-BPV to the USB power  
211 supply. Apart from this instance, switching to  $>5\text{V}$  was not observed at any other time during the  
212 experiment shown in **Figure 2**, indicating that the CPU was powered successfully throughout by  
213 the Al-BPV. The system also incorporated an LED that flashed when the CPU was powered by  
214 the Al-BPV. Failure of the Al-BPV to power the CPU would cause the LED to stop flashing until  
215 the system was reset. Failure was not seen at any time during the experimental run except when  
216 deliberately induced.

217 The current and voltage profile recorded during the six months of testing (**Fig.2D-G**) did not show  
218 consistent decline by the end of the test, and the system was still running on the date of submission  
219 of this manuscript (2022/01/19 - see Channel 1033008 (<https://thingspeak.com/channels/1033008>)  
220 of the ThingSpeak™ platform (**Fig.S11**)). The durability of the compact Al-BPV system was also  
221 demonstrated in a parallel experimental test run for more than four months (**Fig.S12**). This test  
222 was stopped for analysis of the anode and anodic microbiome (see below). A larger prototype has  
223 remained functional for over two years (**Fig.S13**). To our knowledge, this study is the first to report  
224 continuous powering of a microprocessor using a bio-electrochemical system driven by  
225 photosynthetic microorganisms with ambient light as the sole energy input, without the need for  
226 any additional battery, or organic fuel and outside of laboratory-controlled conditions.



228  
 229  
 230  
 231  
 232  
 233  
 234  
 235  
 236  
 237  
 238  
 239  
 240  
 241  
 242  
 243

**Fig. 2. Powering the Arm Cortex-M0+ processor by the compact AI-BPV system in a domestic environment** (from 2021/02/20 to 2021/08/02). The CPU alternated in cycles of 45 minutes of computing mode and 15 minutes of standby. The data presented in the left column (A,D,G,J and M) show the entire experimental run. Central columns (B,E,H,K and N) illustrate insets of two days of recording taken from an arbitrary point (depicted by the gray-shaded regions) of the left column. The data presented in the right column (C,F,I,L and O) show three hours of recording taken from an arbitrary point (depicted by the grey-shaded regions) of the central column. A-C) Cumulative number of cycles of the sum of consecutive integers computed by the CPU. D-F) Electrical current generated by the BPV device. G-I) Absolute potential difference between the anode and cathode of the BPV device. The dotted line indicates the threshold of electric potential below which the processor cannot be powered. J-L) Ambient light measured by a light sensor placed in proximity to the AI-BPV system. M-O) Environmental temperature measured by a temperature sensor integrated into the test-chip board. The red-shaded regions depicted in panels G and M indicate a phase during which the AI-BPV failed to power the CPU induced by deliberately lowering the ambient temperature below 5 C°, as zoomed in Fig.S14).

244  
245  
246  
247  
248  
249  
250  
251  
252  
253  
254  
255  
256  
257  
258  
259  
260  
261  
262  
263  
264  
265  
266  
267  
268  
269  
270  
271  
272  
273  
274  
275

***Working hypothesis for the mechanism of operation of the Al-BPV system***

There are two possible modes of operation for the Al-BPV, which we refer to for simplicity as ‘electrochemical’ and ‘bio-electrochemical’ modes. Although both rely on the photosynthetic activity of the microorganisms in the anodic chamber, in the electrochemical mode, the photosynthetic microorganisms do not directly generate current responsible for the electrical output. Instead, they provide a favourable environment for aluminium oxidation, *e.g.*, through local alkalization, and electrical output stems from current derived from electrochemical aluminium oxidation. In this electrochemical mode the Al-BPV system works as a photosynthetic microbially assisted aluminium air battery (**Fig.3A**). By contrast, in the bio-electrochemical mode, the photosynthetic microorganisms themselves generate the electrons constituting the electrical output of the Al-BPV system. Electron transfer would presumably occur via the outer bacterial membranes through the extracellular matrix to the aluminium, perhaps involving secreted electron shuttles<sup>32</sup> (**Fig.3B**). It is possible that both modes coexist and the predominant mode changes over time.

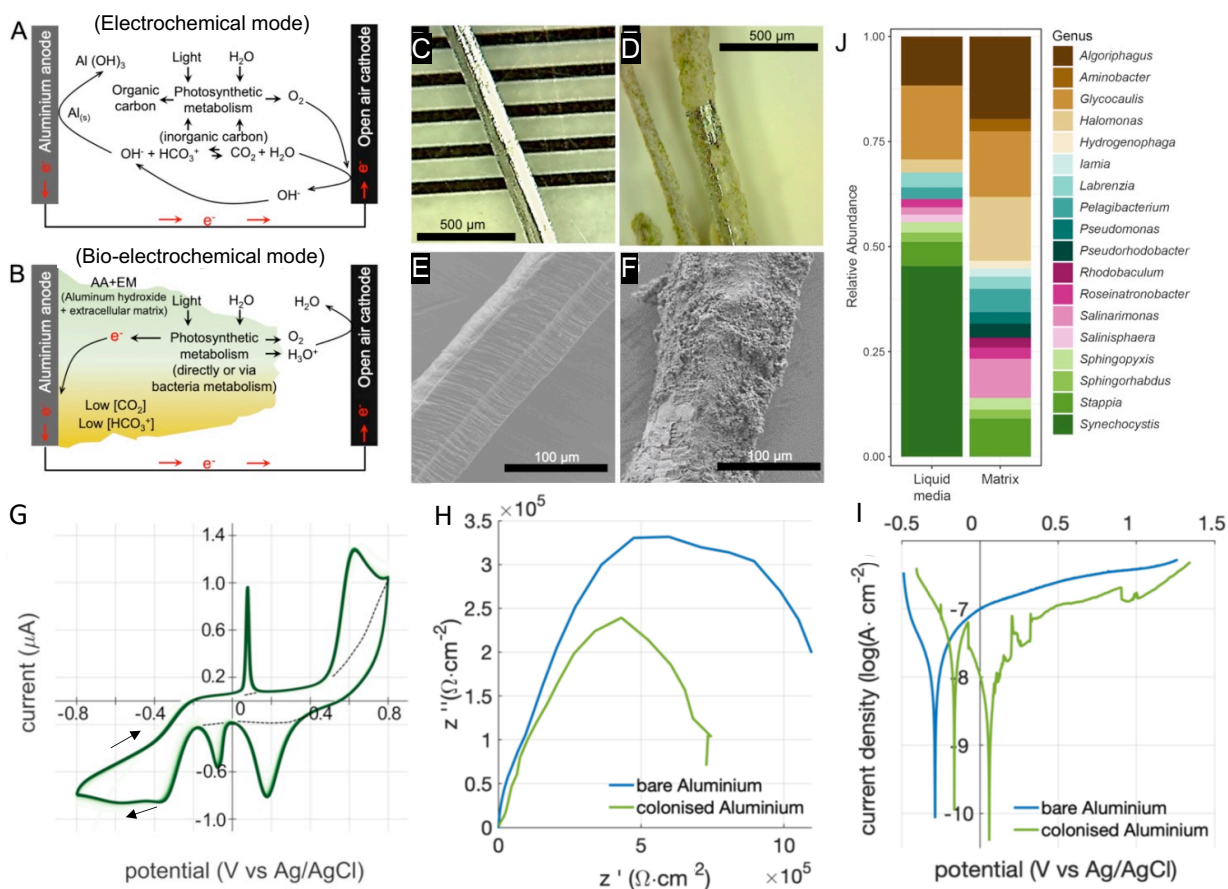
A number of analyses were carried out to assess the importance of the two modes. Optical microscopy and scanning electronic microscopy (SEM) of filaments of aluminium taken from a device that had operated for four months showed a dense layer of material had built up on the anode, possibly including oxidation products and biofilm components (**Fig.3C-F, S15**). This layer, accumulated over time, would be expected to limit further aluminium oxidation. We also carried out cyclic voltammetry (CV) analysis on aluminium hydroxide and extracellular matrix scraped from the anode of a mature Al-BPV system. CVs showed oxidation and reduction peaks indicating the presence of one or more redox active species (**Fig.3G**), which could most readily be explained if they were generated by microorganisms at the anode. Electrochemical impedance spectroscopy (EIS) measurements showed that the  $R_p$  of a bare Al anode was approximately two-fold greater than that of the anode taken from an Al-BPV system four months old (**Fig.3H**). However, a potentiodynamic sweep (PDS) curve (**Fig.3I**) of new aluminium filaments without biofilms submerged in BG11 medium showed only a weak increase of current with potential in the anodic branch (the region with potential increasing from ca. -0.3 V), thus excluding pitting (*i.e.*, fast dissolution of aluminium). The PDS curve of the colonised aluminium (**Fig. 3I**) also did not show a strong current increase in the anodic branch. From these measurements, there is no indication that anodic polarisation would lead to fast corrosion of the aluminium surface in new or colonised

276 filaments, consistent with the fact that although microbially influenced corrosion is known to affect  
277 iron, it is much less common on aluminium<sup>33</sup>. Although bacteria are known to affect aluminium  
278 alloys in chloride-rich environments (*i.e.*, seawater)<sup>34,35</sup>, the mineral medium used in our study had  
279 a low chloride concentration (~0.5 mM), making microbial corrosion less likely.

280 In summary, the amount of material deposited on the anode increased with time, and the  
281 polarization resistance decreased with time. The PDS data indicate that fast corrosion of the  
282 aluminium was not occurring. The decrease of the polarisation resistance may indicate  
283 modification of the aluminium oxide layer by the microorganisms, facilitating electron transfer  
284 through the usually insulating oxide. The persistent current output and photo-response seen in Al-  
285 BPV systems several months old even when the anode was covered with passivating components  
286 suggest the bio-electrochemical mode makes an important contribution to electrical output with  
287 mature systems. A mixed, dynamic scenario, with a change in the relative importance of the two  
288 modes could explain the variation of current output observed during the long-term operation of the  
289 Al-BPV (*e.g.*, **Fig.2.D,G** and **Fig.S12D,G**). The electrical connection of the microorganisms to the  
290 electrode would presumably depend on factors such as their adhesion, the build-up of material on  
291 the electrode, and the production of redox mediators by the microorganisms. These properties  
292 would affect the performance of the device as an energy harvester. For future applications,  
293 microorganisms could be selected to optimize the relevant properties.

294 We also sequenced prokaryotic ribosomal RNA genes from DNA extracted from cells in a  
295 compact-Al-BPV system that had initially been inoculated with cells of the cyanobacterium  
296 *Synechocystis*, but then operated for several months in a non-sterile domestic environment.  
297 Evidence was found for a complex biome containing a wide range of microorganisms, including  
298 representatives of *Halomonas* and *Pseudomonas* (**Fig.3J**), genera which include electroactive  
299 bacteria<sup>36-37</sup>. These microbes might provide redox active electron shuttles (which many  
300 electroactive bacteria are known to do<sup>38</sup>), and/or oxidise organic metabolites received from the  
301 photoautotrophs, transferring electrons to the anode (**Fig.S16**). Having a consortium of  
302 microorganisms in the anode compartment, with photoautotrophs and heterotrophs sharing  
303 different functions, may offer enhanced stability and less susceptibility to contamination<sup>39-40</sup>. The  
304 change in current output seen over time in long-running experiments (*e.g.*, **Fig.2D**) might reflect  
305 a change in microbial composition.

306



307

308 **Fig. 3. Proposed mechanisms of operation of Al-BPV system.** A) Diagram illustrating the  
 309 processes during the proposed electrochemical operational mode. B) Diagram illustrating the  
 310 processes during the proposed bio-electrochemical operational mode. C,D) Optical microscopy of  
 311 new (C) and colonised aluminium anodes (D). E,F) Electron microscopy of new (E) and colonised  
 312 aluminium anodes (F). G) Cyclic voltammety performed on a sample of aluminium hydroxide and  
 313 extracellular components scraped from an aluminium anode taken from an Al-BPV system several  
 314 months old (21 scans at rate of 10 mV s<sup>-1</sup>, Screen-Printed Gold Electrode C223BT. H)  
 315 Electrochemical impedance spectroscopy on a bare aluminium anode in BG11 growth medium  
 316 without microbes (blue trace) and a colonised aluminium anode (green trace). The diameter of the  
 317 semi-circle in the plot corresponds approximately to the polarization resistance R<sub>p</sub>. I)  
 318 Potentiodynamic sweep on bare aluminium anode submerged in BG11 growth medium without  
 319 microbes (blue trace) and colonised aluminium anode (green trace). J) Identification by ribosomal  
 320 RNA sequencing of the prokaryotic microbiome found in the liquid phase and matrix (aluminium  
 321 hydroxide and extracellular components). Sample was taken from an Al-BPV system after four  
 322 months of operation in a domestic environment.

323

324

325

326 **Conclusion**

327 We have developed a novel aluminium-anode biophotovoltaic system (Al-BPV) based on  
328 widespread non-toxic photosynthetic microorganisms (*Synechocystis*) built using common,  
329 durable, inexpensive and largely recyclable materials (**Fig.1C-D, S2, S6-S7**).

330 The compact Al-BPV is comparable in size to an AA battery, and it is capable of powering the  
331 Arm Cortex M0+ processor (**Fig.1F,G** and **Fig.S11**) for more than six months in a domestic  
332 environment without any subsidiary energy storage device, artificial lighting or organic feeding  
333 (**Fig.2**).

334 We propose the Al-BPV system as a practical alternative to PVs and MFCs for powering small  
335 electronic devices for numerous domestic, industrial and agricultural applications, and potentially  
336 in remote locations. Our system has a unique place in the landscape of this technology (**Fig.S17,**  
337 **Table S1**) and paves the way for the development and implementation of a vast number of  
338 photosynthetically-powered IoT devices.

339

340

341 **References and Notes**

342 [1] S. Kumar, P. Tiwari and M. Zymbler, Internet of things is a revolutionary approach for future  
343 technology enhancement: a review. *Journal of Big Data*, 2019, **6**, 111.

344

345 [2] N. Gondchawar and R. S. Kawitkar, IoT-based smart agriculture. *International Journal of*  
346 *Advanced Research in Computer and Communication Engineering*, 2016, **5**, 838-842.

347

348 [3] T. Kim, C. Ramos and S. Mohammed, Smart city and IoT. *Future Generation Computer Sys-*  
349 *tems*, 2017, **76**, 159–162.

350

351 [4] E. Hittinger and P. Jaramillo, Internet of things: Energy boon or bane? *Science*, 2019, **364**,  
352 326–328.

353

354 [5] ARM White Paper: “The route to a trillion devices - the outlook for IoT investment to 2035”,  
355 [https://community.arm.com/cfs-file/\\_key/telligent-evolution-components-attachments/01-1996-  
356 00-00-00-01-30-09/Arm-2D00-The-route-to-a-trillion-devices-2D00-June-2017.pdf](https://community.arm.com/cfs-file/_key/telligent-evolution-components-attachments/01-1996-00-00-00-01-30-09/Arm-2D00-The-route-to-a-trillion-devices-2D00-June-2017.pdf), (ac-  
357 cessed June 2020).

358

359 [6] B.W. Jaskula, Lithium, domestic production and use. Tech. Rep., *National Minerals Infor-*  
360 *mation Center*, 2020, [https://pubs.usgs.gov/periodicals/mcs2020/  
361 mcs2020-lithium.pdf](https://pubs.usgs.gov/periodicals/mcs2020/mcs2020-lithium.pdf).

- 362 [7] J. F. Peters, M. Baumann, B. Zimmermann, J. Braun and M. Weil, The environmental impact  
363 of Li-ion batteries and the role of key parameters – a review. *Renewable and Sustainable Energy*  
364 *Reviews*, 2017, **67**, 491–506.
- 365  
366 [8] J. Curry and N. Harris, Powering the environmental internet of things. *Sensors*, 2019, **19**, 8,  
367 1940.
- 368  
369 [9] R.A. Kjellby, L. R. Cenkeramaddi, T. E. Johnsrud, S. E. Løtveit, G. Jevne, B. Beferull-  
370 Lozano and J. Soumya, Self-powered IoT device based on energy harvesting for remote applica-  
371 tions. *International Symposium on Advanced Networks and Telecommunication Systems*, 2018,  
372 **2018**, 1-4.
- 373  
374 [10] H. Elahi, K. Munir, M. Eugeni, S. Atek and P. Gaudenzi, Energy harvesting towards self-  
375 powered IoT devices. *Energies*, 2020, **13**, 5528.
- 376  
377 [11] H. Michaels, M. Rinderle, R. Freitag, I. Benesperi, T. Edvinsson, R. Socher, A. Gagliardi  
378 and M. Freitag, Dye-sensitized solar cells under ambient light powering machine learning: to-  
379 wards autonomous smart sensors for the internet of things. *Chemical Science*, 2020, **11**, 2895–  
380 2906.
- 381  
382 [12] R. Veerubhotla, S. Nag and D. Das, Internet of things temperature sensor powered by bacte-  
383 rial fuel cells on paper. *Journal of Power Sources*, 2019, **438**, 226947.
- 384  
385 [13] C. Covaci and A. Gontean, Energy harvesting with piezoelectric materials for IoT – review.  
386 *ITM Web of Conferences*, 2019, **29**, 03010.
- 387  
388 [14] S. Castro-Hermosa, G. Lucarelli, M. Top, M. Fahland, J. Fahlteich and T.M. Brown, Perov-  
389 skite photovoltaics on roll-to-roll coated ultra-thin glass as flexible high-efficiency indoor power  
390 generators. *Cell Reports Physical Science*, 2020, **1**, 10045.
- 391  
392 [15] B.E. Logan, B. Hamelers, R. Rozendal, U. Schröder, J. Keller, S. Freguia, P. Aelterman, W.  
393 Verstraete and K. Rabaey, Microbial fuel cells: methodology and technology. *Environmental*  
394 *Science and Technology*, 2006, **40**, 5181–5192.
- 395  
396 [16] A.J. McCormick, P. Bombelli, R.W. Bradley, R. Thorne, T. Wenzel and C.J. Howe, Chris-  
397 topher, Biophotovoltaics: Oxygenic photosynthetic organisms in the world of bioelectrochemical  
398 systems. *Energy and Environmental Science* **8**, 1092–1109 (2015).
- 399  
400 [17] J. Tschörtner, B. Lai and J.O. Krömer, Biophotovoltaics: Green power generation from sun-  
401 light and water. *Frontiers in Microbiology*, 2019, **10**, 866.
- 402  
403 [18] L. T. Wey, P. Bombelli, X. Chen, J. M. Lawrence, C. M. Rabideau, S. J. L. Rowden, J. Z.  
404 Zhang and C. J. Howe, The development of biophotovoltaic systems for power generation and  
405 biological analysis. *ChemElectroChem*, 2019, **6**, 5375–5386.
- 406

- 407 [19] C.J. Howe and P. Bombelli, Electricity production by photosynthetic microorganisms.  
408 *Joule*, 2020, **4**, 2065–2069.
- 409  
410 [20] P. Bombelli, M. Zarrouati, R.J. Thorne, K. Schneider, S.J. Rowden, A. Ali, K. Yunus, P.J.  
411 Cameron, A.C. Fisher, D. Ian Wilson, C.J. Howe and A.J. McCormick, Surface morphology and  
412 surface energy of anode materials influence power outputs in a multi-channel mediatorless bio-  
413 photovoltaic (BPV) system. *Physical Chemistry Chemical Physics*, 2012, **14**, 12221–12229.
- 414  
415 [21] A. Baudler, I. Schmidt, M. Langner, A. Greiner and U. Schröder, Does it have to be carbon?  
416 Metal anodes in microbial fuel cells and related bioelectrochemical systems. *Energy and Envi-  
417 ronmental Science* **8**, 2048–2055 (2015).
- 418  
419 [22] P. Dolara, Occurrence, exposure, effects, recommended intake and possible dietary use of  
420 selected trace compounds (aluminium, bismuth, cobalt, gold, lithium, nickel, silver). *Internat-  
421 tional Journal of Food Sciences and Nutrition*, 2014, **65**, 911–924.
- 422  
423 [23] Y. Liu, Q. Sun, W. Li, K.R. Adair, J. Li and X. Sun A comprehensive review on recent pro-  
424 gress in aluminum–air batteries. *Green Energy and Environment*, 2017, **2**, 246–277.
- 425  
426 [24] A. Rajasekar and Y.P. Ting, Microbial corrosion of aluminum 2024 aeronautical alloy by  
427 hydrocarbon degrading bacteria *Bacillus cereus* ACE4 and *Serratia marcescens* ACE2. *Indus-  
428 trial and Engineering Chemistry Research*, 2010, **49**, 6054–6061.
- 429  
430 [25] J. S. de Andrade, M. R. S. Vieira, S. H. Oliveira, S. K. de Melo Santos and S. L. U. Filho,  
431 Study of microbiologically induced corrosion of 5052 aluminum alloy by sulfate-reducing bacte-  
432 ria in seawater. *Materials Chemistry and Physics*, 2020, **241**, 122296.
- 433  
434 [26] E. Bojórquez-Quintal, C. Escalante-Magaña, I. Echevarria-Machado and M. Martinez-Esté-  
435 vez, Aluminum, a friend or foe of higher plants in acid soils. *Frontiers in Plant Science*, 2017, **8**,  
436 1767.
- 437  
438 [27] M. Ameri, A. Baron-Sola, R.A. Khavari-Nejad, N. Soltani, F. Najafi, A. Bagheri, F. Mar-  
439 tinez and L.E. Hernández, Aluminium triggers oxidative stress and antioxidant response in the  
440 microalgae *Scenedesmus sp.*, *Journal of Plant Physiology*, 2020, **246-247**, 153114.
- 441  
442 [28] J.W. Schultze and M.M. Lohregel, Stability, reactivity and breakdown of passive films.  
443 problems of recent and future research. *Electrochimica Acta*, 2000, **45**, 2499-2513.
- 444  
445 [29] H. Wilson and A. Erbe, Convection induced by illumination-based metal surface heating in-  
446 creases corrosion potential, corrosion rates. *Electrochemistry Communications*, 2019, **106**,  
447 106513.
- 448  
449 [30] K.K. Rao, D.O. Hall, N. Vlachopoulos, M. Grätzel, M.C.W. Evans and M. Seibert, Photoe-  
450 lectrochemical responses of photosystem II particles immobilized on dye-derivatized Ti-O<sub>2</sub>  
451 films. *Journal of Photochemistry and Photobiology, B: Biology*, 1990, **5**, 379–389.
- 452

- 453 [31] ARM. Cortex-M0+ Technical Reference Manual, [https://developer.arm.com/documenta-](https://developer.arm.com/documentation/ddi0484/latest)  
454 [tion/ddi0484/latest](https://developer.arm.com/documentation/ddi0484/latest), (accessed September 2019).  
455
- 456 [32] J. Myers, A. Savanth, R. Gaddh, D. Howard, P. Prabhat and D. Flynn, A Subthreshold ARM  
457 Cortex-M0+ subsystem in 65 nm CMOS for WSN applications with 14 power domains, 10t  
458 SRAM, and integrated voltage regulator. *IEEE Journal of Solid-State Circuits*, 2016, **51**, 31–44.  
459
- 460 [33] A. Savanth, A. Weddell, J. Myers, D. Flynn and B. Al-Hashimi, A 50nW voltage monitor  
461 scheme for minimum energy sensor systems. In *Proceedings - 2017 30th International Confer-*  
462 *ence on VLSI Design and 2017 16th International Conference on Embedded Systems*, 2017,  
463 **2017**, 81–86.  
464
- 465 [34] D. J. Lea-Smith, P. Bombelli, R. Vasudevan and C.J. Howe, Photosynthetic, respiratory and  
466 extracellular electron transport pathways in cyanobacteria. *Biochimica et Biophysica Acta – Bio-*  
467 *energetics*, 2016, **1857**, 247–255.  
468
- 469 [35] B.J. Little, D.J. Blackwood, J. Hinks, F.M. Lauro, E. Marsili, A. Okamoto, S.A. Rice, S.A.  
470 Wade and H.C. Flemming, Microbially influenced corrosion—any progress? *Corrosion Science*,  
471 2020, **170**, 108641.  
472
- 473 [36] M. Tahernia, M. Mohammadifar, Y. Gao, W. Panmanee, D.J. Hassett and S. Choi, A 96-  
474 well high-throughput, rapid-screening platform of extracellular electron transfer in microbial fuel  
475 cells. *Biosensors and Bioelectronics*, 2020, **162**, 112259.  
476
- 477 [37] F. Zeng, Y. Wu, L. Bo, L. Zhang, W. Liu and Y. Zhu, Coupling of electricity generation and  
478 denitrification in three-phase single-chamber MFCs in high-salt conditions. *Bioelectrochemistry*,  
479 2020, **133**, 107481.  
480
- 481 [38] S.W. Li, G. P. Sheng, Y. Y. Cheng and H.Q. Yu, Redox properties of extracellular poly-  
482 meric substances (EPS) from electroactive bacteria. *Scientific Reports*, 2016, **6**, 39098.  
483
- 484 [39] E. Kazamia, D.C. Aldridge and A.G. Smith, Synthetic ecology - a way forward for sustaina-  
485 ble algal biofuel production? *Journal of Biotechnology*, 2012, **162**, 163–169.  
486
- 487 [40] R.L. Shahab, S. Brethauer, M.P. Davey, A.G. Smith, S. Vignolini, J.S. Luterbacher and  
488 M.H. Studer, A heterogeneous microbial consortium producing short-chain fatty acids from lig-  
489 nocellulose. 2020, *Science* **369**, eabb1214.

490

### 491 *Acknowledgments*

492 The authors thank Eystein Vada (NTNU) for technical assistance with SEM.

493

### 494 *Funding*

495 Biotechnology and Biological Sciences Research Council studentship, BB/M011194/1 (to ASc),  
496 National Biofilms Innovation Consortium 02POC19029 (to SJLR)  
497 The Italian Ministry of University and Research (MIUR), within the SIR2014 Grant, project  
498 RBSI14JKU3 (to PB).  
499 Natural Environment Research Council National Capability Science & Facilities funding  
500 NE/R017050/1 and Scottish Association for Marine Science internal research funds (to DHG).

501

502 ***Author contributions (listed alphabetically)***

503 Conceptualization: ASa, CJH, EO, PB

504 Methodology: AE, ASa, CJH, DHG, EO, PB

505 Investigation: ASa, ASc, EÅ, DHG, IJ, PB, SJLR,

506 Visualization: AE, ASa, ASc, DHG, EÅ, EO, IJ, PB

507 Funding acquisition: CJH, DHG, EO, MFH-M, ST

508 Project administration: ASa, CJH, EO

509 Supervision: AE, ASa, CJH, EO, MFH-M

510 Writing – original draft: AE, ASa, ASc, EÅ, IJ, PB, SJLR

511 Writing – review & editing: AE, ASa, ASc, EÅ, EO, CJH, DHG, IJ, MFH-M, PB, SJLR, ST

512

513 ***Competing interests***

514 CJH and PB hold Patent GB2466415 - Hydrogen and electrical current production from  
515 photosynthetically driven semibiological devices.

516

517 ***Data and materials availability***

518 The data that support the plots within this paper and other findings of this study are available at:  
519 <https://doi.org/10.17863/CAM.74822>

520 ***Supplementary Materials:***

521 Figs. S1 to S17

522 Tables S1

523 Materials and Methods